NANOSYSTEMS: PHYSICS, CHEMISTRY, MATHEMATICS, 2015, 6 (6), P. 850–856

Quasi free-standing one-dimensional nanocrystals of PbTe grown in 1.4 nm SWNTs

A. V. Lukashin[1,2], N. S. Falaleev[1], N. I. Verbitskiy[1,3,4], A. A. Volykhov[2], I. I. Verbitskiy[2], L. V. Yashna[2], A. S. Kumskov[5], N. A. Kiselev[5], A. A. Eliseev[1,2]

[1]Department of Materials Science, Moscow State University, 119992, Moscow, Russia
[2]Department of Chemistry, Moscow State University, 119992, Moscow, Russia
[3]Faculty of Physics, University of Vienna, A-1090 Vienna, Austria
[4]Institute of Physics 2, University of Cologne, 50937 Cologne, Germany
[5]Shubnikov Institute of Crystallography RAS, 119333, Moscow, Russia

fnm@fnm.msu.ru

PACS 81.05.U- **DOI 10.17586/2220-8054-2015-6-6-850-856**

Here, we show successful filling of 1.4 nm single-walled carbon nanotubes (SWNT) with PbTe nanocrystals. The structure of one-dimensional PbTe in SWNT was determined using high-resolution transmission electron microscopy (HRTEM). The electronic structure of composites was studied by optical absorbance and Raman spectroscopies indicating no noticeable interaction of encapsulated PbTe with SWNT wall. Experimental data are supported by *ab-initio* calculations, showing non-zero density of states at the Fermi level of PbTe@SWNT(10,10) provided by both SWNT and PbTe states and thus metallic conductivity of the composite.

Keywords: Encapsulated SWNT, SWCNT, quasi free-standing nanocrystals, PbTe@SWCNT, doping, electronic properties, HRTEM, HAADF STEM.

Received: 20 October 2015

Revised: 29 October 2015

1. Introduction

Current progress in microelectronics has nearly attained the extensive miniaturization limit of silicon technology, which necessitates development of new paradigm for semiconductor engineering. One possible pathway to expand the boundaries of traditional silicon technology involves elaboration of nanonowire- and nanotube-based integrated circuits. Most attention is paid to single-walled carbon nanotube (SWNT) based electronics [1, 2]. SWNTs are characterized by their outstanding electrical conductivity [3], extreme mechanical strength [4] and unique electronic structure. They may possess metallic conductivity, or act as wide or narrow gap semiconductor, depending on their chirality and doping level.

It is generally accepted that the electronic structure of SWNTs can be successfully altered by chemical modification of their internal channels. Encapsulation of nanotubes with electron-donor or electron-acceptor compounds allows one to increase or, accordingly, decrease an electron density on nanotube walls [5–7]. This makes it possible to control the electronic properties of SWNTs by intercalating an electron-acceptor or electron-donor substances and even form a p-n junction, for example, in the case of a partially-filled nanotube, which is essential for application in nanoelectronics. Moreover, encapsulation of perfect 1D crystals into nanotube channels enables one to take advantage of specific properties of nanocrystalline materials, including one-dimensional semiconductor, conductive or magnetic nanostructures. SWNTs are known as an atomically smooth and chemically inert template, which protects 1D

nanocrystal from the external influences, and enables one to take advantage of quasi-freestanding inorganic 1D crystals with atomically-designed electronic properties.

The properties of such one-dimensional crystals are known to differ drastically from that of the bulky phases [8]. For instance, band gap expansion has been observed for 1D crystals of SnSe, while a gapless energy spectrum was found for 1D crystals of SnTe [9, 10] or S [11]. It was even possible to detect 1D semiconductor crystal singularities in the electron DOS [9]. However, experimental works on the electronic structure of quasi-free standing nanocrystals are still very rare, which restricts the formulation of the general principles for the design of electronic properties for 1D nanocrystals on an atomic level.

The electronic structure of X@SWNT composite materials is known to be governed by the work function difference of SWNT and guest crystals [12]. To minimize crystal interaction with the SWNT, one needs to equalize the work functions of the guest compound to that of the SWNTs. Among others, PbTe with $\varphi = 4.52$ eV looks to be a promising candidate for growing quasi free-standing nanocrystals inside SWNTs. Therefore, in the present study we have focused on synthesis of PbTe@SWNT composites and determination of their atomic arrangement and electronic structure using HRTEM, optical absorption and Raman spectroscopies. Experimental data are supported by *ab-initio* calculation, showing metallic type of conductivity in the obtained nanostructures.

2. Experimental

SWNT were synthesized by the catalytic arc-discharge method using Y/Ni powder catalyst (atomic ratio 1:4) at 550 Torr helium pressure and electric current of 100 – 110 Å on 0.8 – 1.0 cm diameter graphite electrodes. The synthesized nanotubes were purified by a multistage purification process, which consisted of oxygen treatment at 350 – 400 °C and rinsing with HCl to remove the remaining catalyst. Then, SWNT were opened by aerobic treatment at 500 °C over 30 mins. Pre-opened nanotubes were filled using capillary technique. SWNTs were mixed with PbTe (Aldrich, 99.998 %) (mass ratio 1:10) and crushed in an agate mortar. The mixture was evacuated to a pressure of 10 – 5 mbar and sealed in a quartz ampule. The mixture in the ampule was treated at 1024 °C for 6 hours, which lead to filling of nanotubes with PbTe melt. Subsequent cooling at 0.1 °C/min to 944 °C, 0.02 °C/min to 904 °C and 0.1 °C/min to 824 °C resulted in formation of 1D PbTe crystals in the nanotube channels.

High-resolution transmission electron microscopy (HRTEM) was performed with FEI Titan 80 – 300 and Zeiss Libra 200 electron microscopes with a spherical/chromatic aberration correction. The samples were dispersed onto lacey carbon-coated grids. Optical absorption spectra were acquired using PerkinElmer Lambda 950 UV/Vis/NIR spectrophotometer with a spectral resolution of 1 nm. Raman spectroscopy was performed on a Renishaw InVia Raman spectroscope (based on a Leica DMLM microscope equipped with 100× lens) using a 20-mW 514-nm argon laser, a 17-mW 633-nm HeNe laser, and a 300-mW 785-nm NIR diode laser, variable power ND filters (power range 0.00005 – 100 %) and near-excitation tunable (NeXT) filters. A CCD camera with resolution 1024×532 pixels was used as a sensor. The resonance lines positions in the spectra were determined by least-squares fitting of experimental data by Voight function using WiRE 3.1 software. All Raman spectra were acquired at room temperature.

Ab-initio calculations were performed using Vienna *ab-initio* simulation package (VASP) software. The PAW-potential (Projector Augmented Wave potential) was used and the exchange-correlation energy was treated in a GGA (generalized gradient approximation). The first Brillouin zone integrations were made using Monkhorst and Pack approximation [13];

10 – 50 k-points were used for calculation. Plane-wave cut-off energies were chosen to be 400 eV.

3. Discussion

HRTEM is a powerful method to study structure of such systems, however, the high locality of this technique should be considered. For this reason, a large number of images were taken and analysis was performed for a total nanotube length of over 1000 nm. Fig. 1 shows the microphotograph of single SWNT filled with PbTe. The capillary technique resulted in successful encapsulation of PbTe and formation of a quasi-one-dimensional crystal inside the inner channel. According to statistical analysis, the composites are characterized by $\sim$ 80 % loading factor (i.e. the ratio between the filled internal space and the total internal volume), and over 70 % crystallization factor (the fraction of filled nanotubes with a well-defined structure). These high numbers give evidence for the high efficiency of the chosen technique to produce PbTe quasi-one-dimensional crystals.

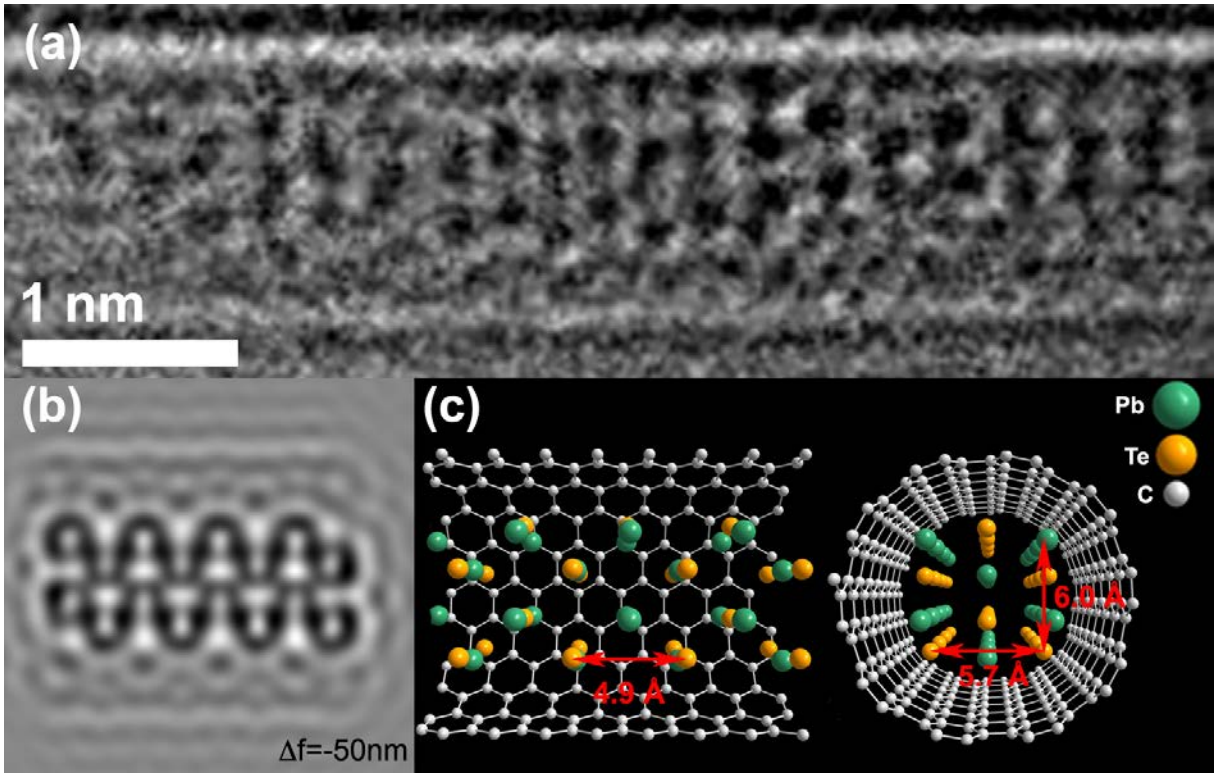

FIG. 1. HRTEM image of PbTe@SWNT (10,10) (a), simulated image (b) and calculated structure model (c)

Further analysis of HRTEM data allowed us to unveil atomic structure of encapsulated PbTe nanocrystals. The crystal periodicity along tube was found equal to be 5.0 Å, and the distance between edging atomic columns equals 6.1 Å. It is known that bulk PbTe crystallizes in a cubic rock salt structure. Taking this fact into account, and the diameter of SWNT of 1.4 nm the structure of the encapsulated crystal was suggested. This structure possesses 6 atoms in the cross-section and 12 atoms in the unit cell and can be derived by cutting the bulk structure along the $\langle 110 \rangle$ direction. The obtained structure was introduced into the inner channel of (10,10) SWNT and geometry of the whole system was optimized in VASP software package. The geometry of the resulting structure was verified by image simulation using SimulaTEM software.

The model fits well the experimental data. According to DFT modeling, encapsulation causes slight deformation of the crystal, which can be seen as slightly modified interatomic distances as compared to the bulk structure. The interatomic Pb-Te distance in bulk PbTe is 3.23 Å. Upon intercalation it changes to 2.97 Å along the nanotube axis, and 2.91 Å in the cross-section, as it is shown in Fig. 1. Such deformation can be caused by undercoordination of 1D crystal atoms. Notably, such compression will necessarily result in a change of the electronic structure of 1D nanocrystal compared to the bulk state.

An average diameter of the tubes obtained by HRTEM measurements (1.4 nm) is well supported by the optical absorption data, shown in Fig. 2. Peaks in the optical absorption spectrum correspond well with the allowed transitions between van Hove singularities of 1.4 – 1.6 nm semiconductor and metallic nanotubes [14]: 0.6 – 0.8 eV (E_{11}^S transition), 1.0 – 1.4 eV (E_{22}^S transition), 1.7 – 2.0 eV (E_{11}^M transition) and 2.3 – 2.5 eV (E_{33}^S transition). To analyze the structure of pristine SWNTs, Raman spectroscopy was employed (Fig. 3). According to optical spectroscopy, 785 nm (1.58 eV) irradiation resonantly excites E_{11}^M transition of metallic nanotubes with 1.5 – 1.6 nm diameter, 633 nm (1.96 eV) laser resonantly excites E_{11}^M transition of $\sim$ 1.4 nm metallic nanotubes and $\sim$ 1.6 nm semiconducting nanotubes, and exposure to 514 nm (2.41 eV) laser leads to resonant excitation of E_{33}^S transition of semiconducting tubes in the sample. The corresponding Raman spectra are shown in Fig. 3. Detailed analysis of obtained spectra, including SWNT chirality sets present the studied sample as derived from RBM- and G-modes positions is presented in Table 1.

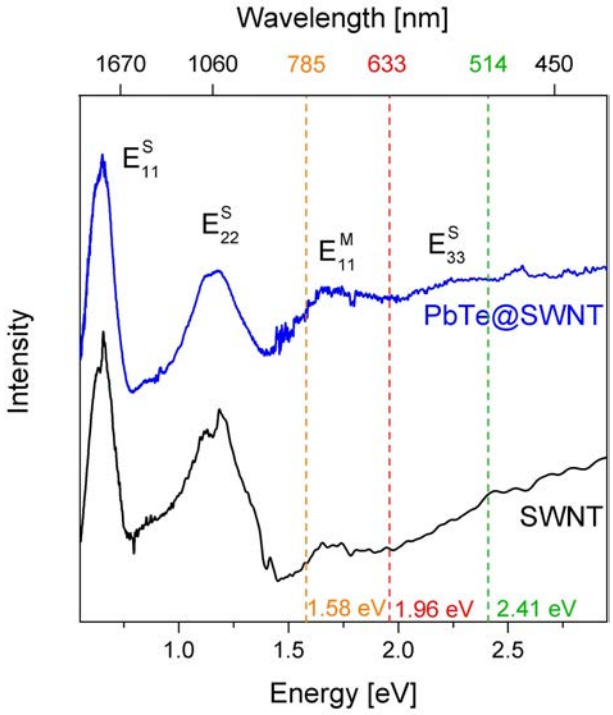

FIG. 2. Optical absorption spectra of pristine SWNT and PbTe@SWNT. Dashed lines indicate excitation laser energy used in Raman spectroscopy

Optical absorption data for PbTe@SWNT composites reveal no significant effect of PbTe intercalation on the electronic structure of SWNTs. No detectable energy shifts of the allowed transitions between van Hove singularities or intensity redistribution were observed, which points towards the possibility of electronic structure description in the framework of the rigid band structure model. Moreover, this also indicates that Fermi level shift does not exceed

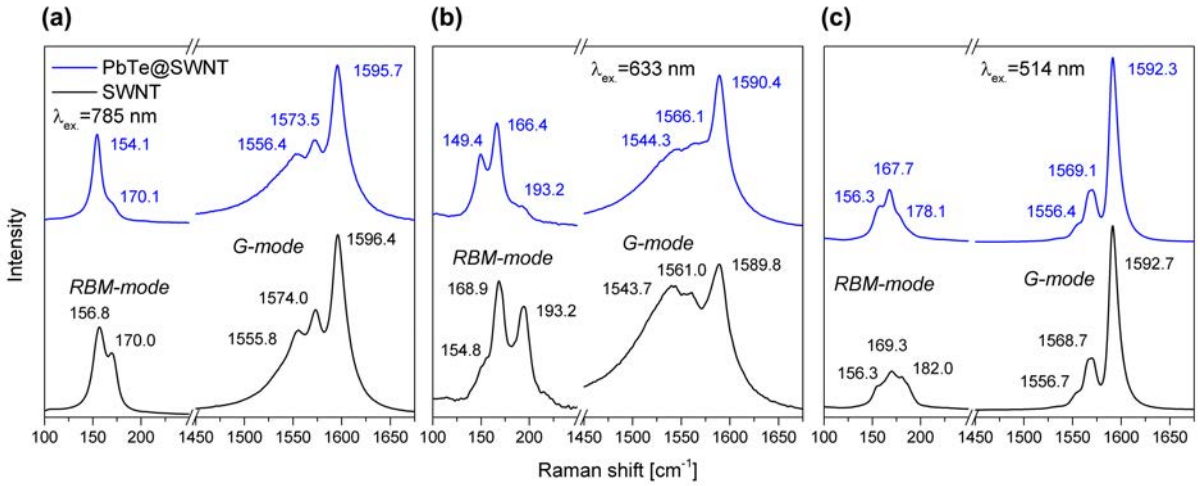

FIG. 3. Raman spectra of pristine SWNT and PbTe@SWNT obtained with 785 nm, 633 nm and 514 nm laser excitation

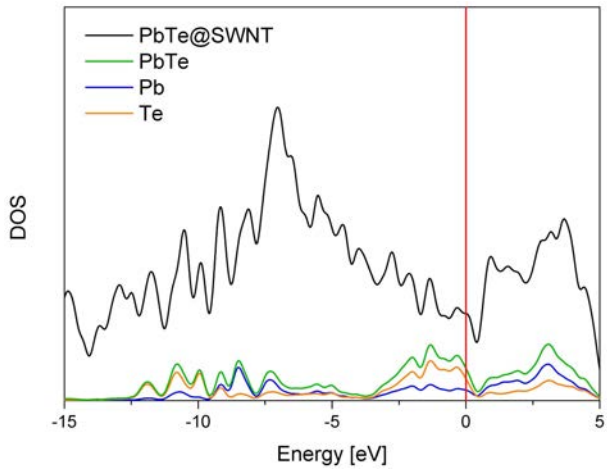

FIG. 4. Calculated density of states of PbTe 1D crystal inside (10,10) SWNT. Red line indicates Fermi level

0.3 eV (first van Hove singularity). Raman spectra acquired at 785 nm, 633 nm and 514 nm laser excitation wavelengths show only slight modification of RBM- and G-band frequencies (Table 2), illustrating no change of resonant excitation conditions and weak interaction between intercalated PbTe crystal and SWNT. It should be noted, that Raman spectra of resonantly excited metallic tubes (633 and 785 nm excitation, Fig. 3a, b) in PbTe@SWNT sample also shows typical 'metallic' G-band profile, while the effect on the metallic tubes is known to be most pronounced in the Raman spectra of doped SWNTs [15, 16]. This points towards the metallic conductivity of PbTe@m-SWNTs. The obtained data suggest the absence of chemical bonding between guest PbTe crystal and nanotube and formation of quasi-free-standing PbTe nanocrystal inside SWNT. Similar behavior was observed early for nanotubes filled with SnTe [9].

The obtained experimental data was supported by *ab-initio* calculations. No significant SWNT-PbTe interactions or localized states were obtained by modeling from C1*s* chemical shifts of carbon atoms. This is in line with earlier percularities of SWNT guest crystal interactions due to work function difference [12]. Density of the electronic states near Fermi level was derived for the optimized structure (Fig. 1b,c). Resulting DOS for PbTe@SWNT(10;10) composite

TABLE 1. Structural parameters of raw SWNT according to the Raman spectroscopy

Excitation energy [eV]	**Dominant ω_{RBM} [cm^{-1}]**	**ω_{G+} [cm^{-1}]**	**Nanotube diameter [nm]**	**Nanotube type**	**Possible chiralities**
1.58	156.8*	1555.8	1.45	*m*–SWNT	(14, 7)*, (16, 4), (15, 6)
	170.0	1574.0 1596.4	1.33	*s*–SWNT	(13, 6)*, (10, 9)*, (14, 4)
1.96	154.8	1543.7	1.47	*m*–SWNT	(15, 6)*, (16, 4)* , (12, 9)
	168.9*	1561.0 1589.8	1.34	*m*–SWNT	(15, 3)*, (16, 1) *, (11, 8)
2.41	156.3	1556.7	1.46	*s*–SWNT	(11, 10)*, (15, 5), (14, 6)
	169.3*	1568.6	1.34	*s*–SWNT	(13, 6)*, (12, 7)*, (10, 9)
	182.0	1592.2	1.24	*s*–SWNT	(15, 1)*, (12, 5), (11, 6)

* Predominantly excited SWNTs

TABLE 2. Positions of the RBM- and G-lines in the Raman spectra of pristine SWNTs and PbTe@SWNT composites aquired at different excitation laser wavelength. The shifts of the peak positions are given in parentheses

Sample	**Excitation energy [eV]**	**Dominant ω_{RBM} [cm^{-1}]**	**Possible SWNT diameter and type**	**$\omega_{G+}(\Delta\omega_{G+})$ [cm^{-1}]**		
SWNT	1.58	156.8	1.45 nm *m*–SWNT	1555.8	1574.0	1596.4
PbTe@SWNT		154.1 (-2.7)	1.48 nm *m*–SWNT	1551.7 (-4.1)	1572.0 (-2)	1596.4 (0)
SWNT	1.96	168.9	1.34 nm *m*–SWNT	1543.7	1561.0	1589.8
PbTe@SWNT		166.4 (-2.5)	1.36 nm *m*–SWNT	1544.3 (+0.6)	1566.1 (+5.1)	1590.4 (+0.5)
SWNT	2.41	169.3	1.33 nm *s*–SWNT	1556.7	1568.6	1592.2
PbTe@SWNT		167.7 (-1.6)	1.33 nm *s*–SWNT	1556.4 (-0.3)	1569.1 (+0.5)	1592.3 (+0.3)

illustrates a non-zero density of states at the Fermi level position (Fig. 4). It should be noted that not only m-SWNT states contribute total DOS at Fermi level but also 1D PbTe, which conforms one-dimensional nanocrystal metallic character.

4. Conclusion

Single-walled carbon nanotubes filled with PbTe were synthetized using capillary filling of pre-opened SWNTs from melt and subsequent slow cooling. HRTEM study showed high efficiency of chosen technique which results in high loading and crystallinity factors. Structure of intercalated PbTe 1D crystal was studied using HRTEM and was found to correspond bulk

PbTe crystal cut along ⟨110⟩ direction. Slight compression of Pb-Te distances was observed in 1D nanocrystal as compared to bulk structure due to undercoordination of 1D crystal atoms. Electronic structure of PbTe@SWNT composite studied by an optical absorption and Raman spectroscopies showed no notable interaction of guest PbTe crystal with SWNT walls, which points towards the formation of quasi-free-standing 1D PbTe crystal inside SWNT. Experimental data are supported by *ab-initio* calculations for PbTe@SWNT(10,10) structure which show non-zero density of states at the Fermi level with contribution from both PbTe and SWNT, revealing the metallic conductivity of PbTe@SWNT.

Acknowledgements

SWNTs were synthesized at the Institute of Problems of Chemical Physics, RAS, Chernogolovka, Russia by A. V. Krestinin. The VASP program package calculations were performed using the SKIF MSU 'Chebyshev' and 'Lomonosov' supercomputers. This work was supported by Russian Science Foundation (Grant No. 14-13-00747).

References

[1] P.G. Collins, H. Bando, A. Zettl. Nanoscale electronic devices on carbon nanotubes. *Nanotechnology*, 1998, **9** (3), P. 153–157.
[2] L. Chico, V.H. Crespi, et al. Pure Carbon Nanoscale Devices: Nanotube Heterojunctions. *Phys. Rev. Lett.*, 1996, **76** (6), P. 971–974.
[3] T.W. Ebbesen, H.J. Lezec, et al. Electrical conductivity of individual carbon nanotubes. *Nature*, 1996, **382**, P. 54–56.
[4] M.M.J. Treacy, T.W. Ebbesen, J.M. Gibson. Exceptionally high Young's modulus observed for individual carbon nanotubes. *Nature*, 1996, **381** (6584), P. 678–680.
[5] P. Chaturvedi, P. Verma, et al. Carbon Nanotube–Purification and Sorting Protocols. *Def. Sci. J.*, 2008, **58** (5), P. 591–599.
[6] M. Weissmann, G. Garca, et al. Theoretical study of iron-filled carbon nanotubes. *Phys. Rev. B*, 2006, **73**, (12), P. 125435.
[7] M. Mahmudur Rahman, M. Kisaku, et al. Electric and Magnetic Properties of Co-filled Carbon Nanotube. *J. Phys. Soc. Jpn.*, 2005, **74** (2), P. 742–745.
[8] A.S. Kumskov, V.G. Zhigalina, et al. The structure of 1D and 3D CuI nanocrystals grown within 1.5 – 2.5 nm single wall carbon nanotubes obtained by catalyzed chemical vapor deposition. *Carbon*, 2012, **50** (12), P. 4696–4704.
[9] L.V. Yashina, A.A. Eliseev, et al. Growth and Characterization of One-Dimensional SnTe Crystals within the Single-Walled Carbon Nanotube Channels. *J. Phys. Chem. C*, 2011, **115** (9), P. 3578–3586.
[10] A.S. Kumskov, A.A. Eliseev, B. Freitag, N.A. Kiselev. HRTEM of 1DSnTe@SWNT nanocomposite located on thin layers of graphite. *J. Microsc.*, 2012, **248** (2), P. 117–119.
[11] T. Fujimori, A. Morelos-Gmez, et al. Conducting linear chains of sulphur inside carbon nanotubes. *Nat. Commun.*, 2013, **4**, P. 2162.
[12] A. Eliseev, L. Yashina, M. Kharlamova, N. Kiselev. One-Dimensional Crystals inside Single-Walled Carbon Nanotubes: Growth, Structure and Electronic Properties. In *Electronic Properties of Carbon Nanotubes*, ed. by J. M. Marulanda, InTech, 2011.
[13] H.J. Monkhorst, J.D. Pack. Special points for Brillouin-zone integrations. *Phys. Rev. B*, 1976, **13** (12), P. 5188–5192.
[14] H. Kataura, Y. Kumazawa, et al. Optical properties of single-wall carbon nanotubes. *Synthetic Metals*, 1999, **103** (1), P. 2555–2558.
[15] S. Piscanec, M. Lazzeri, et al. Optical phonons in carbon nanotubes: Kohn anomalies, Peierls distortions, and dynamic effects. *Phys. Rev. B*, 2007, **75** (3), P. 035427.
[16] A.A. Eliseev, L.V. Yashina, et al. Interaction between single walled carbon nanotube and 1D crystal in CuX@SWCNT (X = Cl, Br, I) nanostructures. *Carbon*, **50** (11), P. 4021–4039.